

Characterization of Two Type 1 Cu Sites of *Hyphomicrobium denitrificans* Nitrite Reductase: A New Class of Copper-Containing Nitrite Reductases[†]

Kazuya Yamaguchi,[‡] Kunishige Kataoka,[§] Mayuko Kobayashi,[‡] Koushi Itoh,[‡] Atsushi Fukui,[‡] and Shinnichiro Suzuki^{*‡}

Department of Chemistry, Graduate School of Science, Osaka University, Toyonaka, Osaka 560-0043, Japan, and Department of Chemistry, Faculty of Science, Kanazawa University, Kakuma, Kanazawa 920-1192, Japan

Received April 14, 2004; Revised Manuscript Received August 1, 2004

ABSTRACT: We report (1) the amino acid sequence of *Hyphomicrobium denitrificans* nitrite reductase (HdNIR), containing two type 1 Cu sites and one type 2 Cu site; (2) the expression and preparation of wild-type HdNIR and two mutants replacing the Cys ligand of each type 1 Cu with Ala; and (3) their spectroscopic and functional characterization. The open-reading frame of 50-kDa HdNIR is composed of the 15-kDa N-terminal domain having a type 1 Cu-binding motif like cupredoxins and the 35-kDa C-terminal domain having type 1 Cu-binding and type 2 Cu-binding motifs such as common nitrite reductases (NIRs). Moreover, the amino acid sequences of the N- and C-terminal domains are homologous to those of plastocyanins and NIRs, respectively. The point mutation of the Cys ligand of each type 1 Cu with Ala gives two mutants, C114A and C260A, possessing one type 1 Cu and one type 2 Cu. The spectroscopic data of C114A reveal that the C-terminal NIR-like domain has the green type 1 Cu (type 1 Cu_C), showing two intense absorption peaks at 455 ($\epsilon = 2600 \text{ M}^{-1} \text{ cm}^{-1}$) and 600 nm ($\epsilon = 2800 \text{ M}^{-1} \text{ cm}^{-1}$) and a rhombic EPR signal like those of the green type 1 Cu of *Achromobacter cycloclastes* NIR (AcNIR). The spectroscopic data of C260A elucidate that the N-terminal Pc-like domain in HdNIR contains the blue type 1 Cu (type 1 Cu_N), exhibiting an intense absorption band at 605 nm ($\epsilon = 2900 \text{ M}^{-1} \text{ cm}^{-1}$) and an axial EPR signal like those of the blue type 1 Cu of *Alcaligenes xylosoxidans* NIR (AxNIR). The sum of the visible absorption or EPR spectra of C114A and C260A is almost equal to the corresponding spectrum of wild-type HdNIR. The spectroscopic characterization of the type 1 Cu indicates that the geometries of the type 1 Cu_N and Cu_C sites are slightly distorted tetrahedral (or axially elongated bipyramidal) and flattened tetrahedral, respectively. In the cyclic voltammograms, the midpoint potentials ($E_{1/2}$), probably because of the type 1 Cu ions of C114A and C260A, are observed at +321 and +336 mV versus normal hydrogen electrode (NHE) at pH 7.0, respectively. These values, which are close to each other, are more positive than those ($\sim +0.24$ – 0.28 V at pH 7.0) of the type 1 Cu sites of AcNIR and AxNIR. The electron-accepting capability of C114A from cytochrome c_{550} is almost similar to that of wild-type HdNIR, whereas that of C260A is very low. This suggests that the type 1 Cu_C in the C-terminal domain is essential for the enzyme functions of HdNIR.

Denitrification is the dissimilatory reduction of nitrate or nitrite usually to dinitrogen in prokaryotic organisms to synthesize ATP, and it is comprised of anaerobic reduction processes, $\text{NO}_3 \rightarrow \text{NO}_2 \rightarrow \text{NO} \rightarrow \text{N}_2\text{O} \rightarrow \text{N}_2$. These processes are caused in either the cytoplasmic membrane or periplasm by the corresponding oxidoreductases containing transition-metal ions (1). Dissimilatory nitrite reductases located in the periplasm catalyze one-electron reduction of nitrite to nitric oxide. Generally, copper-containing nitrite reductases (NIRs)¹ are a trimer, in which a monomer (ca. 37 kDa) contains one type 1 Cu and one type 2 Cu (2–4). The type 1 Cu ligated by four amino acid residues (two His,

one Cys, and one Met) is bound to one of the two β -barrel domains inside the monomer. The type 2 Cu site that has three His ligands and a solvent ligand is bound to the interface between two adjacent monomers, and it is located at the bottom of a ca. 13-Å deep cleft through which the substrate can enter. The distance between the two Cu sites connected through the sequence segment (-Cys-His-) is ca. 12.5 Å (4, 5). The enzyme receives one electron at the type 1 Cu site from an electron donor protein and catalyzes one

[†] This work was supported by Natural Science Research Assistance, Area 1, Specific Research Assistance B from the Asahi Glass Foundation.

^{*} To whom correspondence should be addressed. Telephone: +81-6-6850-5767. Fax: +81-6-6850-5785. E-mail: bic@ch.wani.osaka-u.ac.jp.

[‡] Osaka University.

[§] Kanazawa University.

¹ Abbreviations: NIR, copper-containing nitrite reductase; HdNIR, NIR from *Hyphomicrobium denitrificans* A3151; AcNIR, NIR from *Achromobacter cycloclastes*; AxNIR, NIR from *Alcaligenes xylosoxidans*; C114A, mutant HdNIR replaced Cys114 with Ala; C260A, mutant HdNIR replaced Cys260 with Ala; type 1 Cu_N, the type 1 Cu in plastocyanin-like domain of HdNIR; type 1 Cu_C, the type 1 Cu in NIR-like domain of HdNIR; Pc, plastocyanin; CBP, cucumber basic protein; Cyt c_{550} , cytochrome c_{550} ; SDS, sodium dodecyl sulfate; PAGE, polyacrylamide gel electrophoresis; HPLC, high-performance liquid chromatography; CD, circular dichroism; EPR, electron paramagnetic resonance; RR, resonance Raman; NHE, normal hydrogen electrode.

electron reduction of NO_2^- to NO at the type 2 Cu site. Moreover, a hydrogen-bond network including Asp and His around the type 2 Cu plays an important role in the proton donation to the substrate (6).

We have already reported the spectroscopic and functional characterization of a unique NIR from *Hyphomicrobium denitrificans* A3151 (HdNIR) (7, 8). The electronic absorption, circular dichroism (CD), and electron paramagnetic resonance (EPR) spectra of HdNIR suggested that the subunit has two type 1 Cu sites and one type 2 Cu site. The apparent first-order rate constant (k_{intra}) of the intramolecular electron-transfer reaction from the type 1 Cu to the type 2 Cu in the HdNIR was $2.4 \times 10^{-2} \text{ s}^{-1}$ at pH 6.0 in the presence of the nitrite ion (8). This value is much smaller than those of AxNIR (NIR from *Alcaligenes xylosoxidans*) and AcNIR (NIR from *Achromobacter cycloclastes*) ($k_{\text{intra}} = \sim 1.9\text{--}2.0 \times 10^3 \text{ s}^{-1}$ at pH 6.0) (2, 3). However, the intermolecular electron-transfer rate constant (k_{inter}) of cognate basic cytochrome c_{550} (Cyt c_{550}) to HdNIR was estimated to be $3.7 \times 10^5 \text{ M}^{-1} \text{ s}^{-1}$ at pH 5.5 and 25 °C by cyclic voltammetry. It was similar to those of AcNIR and AxNIR from pseudoazurin ($k_{\text{inter}} = 7.3 \times 10^5 \text{ M}^{-1} \text{ s}^{-1}$ at pH 7.0) (9) and Cyt c_{551} ($k_{\text{inter}} = 4.0 \times 10^5 \text{ M}^{-1} \text{ s}^{-1}$ at pH 6.0) (10), respectively.

HdNIR has been proteolyzed to two protein fragments (14 and 35 kDa) with subtilisin (11). The blue 14-kDa protein fragment [plastocyanin (Pc)-like protein fragment] from Asp1 to Lys139 shows a visible absorption spectrum possessing an intense band at 602 nm and an axial EPR signal, while the green 35-kDa protein fragment (NIR-like protein fragment) from Ser140 to Gln447 exhibits two intense absorption bands at 454 and 597 nm and a rhombic EPR signal. These findings suggested that each fragment has a type 1 Cu; the Pc-like protein fragment contains the blue type 1 Cu that has a slightly distorted tetrahedral or an axially elongated trigonal bipyramidal geometry, and the NIR-like protein fragment contains the green type 1 Cu that has a flattened tetrahedral geometry and also the type 2 Cu. The latter fragment has nitrite reduction activity a little higher than that of native HdNIR. The midpoint potentials of the two type 1 Cu sites are similar to each other, showing +345 and +353 mV [versus normal hydrogen electrode (NHE) at pH 7.0] for the blue type 1 Cu and the green type 1 Cu, respectively. In addition, the intermolecular electron-transfer rate constant for the NIR-like protein fragment from Cyt c_{550} is almost the same as that of the native enzyme. Therefore, the NIR-like domain of HdNIR is necessary for the intermolecular electron transfer and catalytic reactions of the enzyme.

Here, we report the construction of an expression system for HdNIR and specific mutation at the Cys114 or Cys260 ligand of the type 1 Cu site to shed light on the spectral properties, coordination structures, and functions of the two type 1 Cu sites. This work has confirmed that HdNIR is a new class of NIRs.

EXPERIMENTAL PROCEDURES

Materials. The vectors, pUC19 and pQE32, were purchased from Takara Biochemicals and QIAGEN, respectively. *Taq* DNA polymerase, restriction endonucleases, and other modifying enzymes were obtained from Takara Bio and TOYOBO. DIG DNA labeling and detection kit (Roche) and *Taq* dye-terminator cycle sequencing kit (Applied

Biosystems) were used for hybridization and sequence determination, respectively. All other chemicals were of analytical grade.

Isolation and Sequencing of Peptide Fragments. HdNIR (2 mg) purified from the cell extract of *H. denitrificans* (12) was treated with BrCN (25 mg) at 37 °C for 20 h in an aqueous solution of 70% formic acid. The peptide mixture was separated with a Cosmosil 5C18 reverse-phase column (Nacalai Tesque) using an aqueous solution of 0.1% trifluoroacetic acid and a 90% acetonitrile aqueous solution of 0.1% trifluoroacetic acid. High-performance liquid chromatography (HPLC) was carried out at a flow rate of 1.0 mL/min by continuous monitoring of the 215-nm absorbance. The sequences of the peptide fragments were determined with an Applied Biosystems Model 477A protein sequencer.

Cloning of NIR Gene. Two mixed oligonucleotide primers, P1 [5'-CTSCNGCIATGAARGAYAA-3' synthesized on the base of N-terminal sequence (L-P-A-M-K-D-K) of the purified enzyme] and P2 [5'-AARTCNACISWYTGNCAT-3' synthesized on the base of amino acid sequence (M-V-H-S-V-D-F) of the obtained peptide] were employed for polymerase chain reaction (PCR) with the *H. denitrificans* genomic DNA as a template. A fragment with ca. 700-bp thus amplified was labeled with digoxigenin and used for the screening of a partial genomic library. The genomic library was made from 5 to 6-kbp *Hind*III-digested *H. denitrificans* genome DNA fragments inserted into the vector pUC19. A 5.5-kbp DNA inserted in the positive clone (designated as pUHdNIR) by colony hybridization was subjected to sequence determination. DNA sequence analyses were carried out in both directions by the dideoxy chain termination method with an Applied Biosystems Model 373A DNA sequencer.

Construction of Expression Plasmid. A 1.4-kbp gene fragment consisting of a structural gene of HdNIR, *Bam*HI linker, and *Pst*I linker were amplified by PCR using pUHdNIR as a template and two primers [P3, 5'-CCGC-CCCTGGATCCGATGCTCCGGCCATG-3' coding for the N-terminal region of HdNIR and the *Bam*HI digestion sequence (underline); and P4, 5'-GACTCTGCAGGACGCTACTGCTT-CG-3' containing the termination codon and the *Pst*I digestion sequence (underline)]. The PCR products were digested with *Bam*HI and *Pst*I and subcloned into expression plasmid pQE-32 digested with *Bam*HI and *Pst*I to yield pQHdNIR2. The inserted gene was confirmed by DNA sequencing.

Expression and Purification of Recombinant HdNIR. For the expression of HdNIR, we used the QIA express (His)₆-tagged protein expression system (QIAGEN). We have inserted the gene coding for the mature HdNIR to the *Bam*HI site of pQE-32. The resulting plasmid (pQHdNIR2) expressed the His-tagged fusion protein, in which the N-terminal Asp residue is preceded by 12 residues (M-R-G-S-(H)₆-G-S-). With pQHdNIR2, a large amount of the recombinant HdNIR was expressed in *Escherichia coli*.

E. coli JM109 cells carrying pQHdNIR2 were cultured in LB medium supplemented with 1 mM $\text{CuCl}_2 \cdot 2\text{H}_2\text{O}$ and 100 mg/mL sodium ampicillin for 15 h at 37 °C with reciprocal shaking. The cells were harvested and disrupted by sonication in a 50 mM sodium phosphate buffer (pH 8.0) containing 300 mM NaCl and 10 mM imidazole. The cell extract was passed through a Ni-NTA agarose (QIAGEN) column

equilibrated with the same buffer to bind the His-tagged recombinant proteins. After the column was washed, the recombinant protein was eluted with a 50 mM sodium phosphate buffer (pH 8.0) containing 300 mM NaCl and 250 mM imidazole. The recombinant protein was further purified with a RESOURCE Q column (Amersham Biosciences) equilibrated with 50 mM Tris-HCl (pH 7.5). The recombinant protein was eluted with a linear gradient of NaCl (0–0.3 M) in the same buffer. The purified recombinant protein (ca. 10 mg) was obtained from ca. 5 g of wet cells (1 l culture media). The recombinant was reconstituted with $\text{CuSO}_4 \cdot 5\text{H}_2\text{O}$ (1 mM) by overnight dialysis against 20 mM Tris-HCl buffer (pH 7.5) at 4 °C, as described in the previous method (13). The spectroscopic, electrochemical, and enzymatic properties of wild-type HdNIR were indistinguishable from those of native HdNIR.

The ratios of the type 1 Cu to the type 2 Cu in the wild-type and mutant enzymes were estimated as follows. The total copper content of the enzymes reconstituted with Cu^{II} ion was measured with an atomic absorption spectrometer. The protein concentrations of the recombinant and mutants were determined by using BCA Protein Assay Reagent Kit (Pierce, Rockford, IL). Bovine serum albumin was used for the calibration curves. Because it was spectroscopically ascertained that the reconstituted enzymes stoichiometrically contain the type 1 Cu, the concentration of the type 1 Cu is equal to that of the subunit. Therefore, the concentration of the type 2 Cu was obtained by subtracting that of the type 1 Cu from the total copper content. The ratio of the type 1 Cu to the type 2 Cu per one subunit of wild-type HdNIR was estimated to be 2:0.6.

Mutagenesis. The mutations Cys114Ala and Cys260Ala were performed by the two-step PCR method using pQHdNIR2 as a template and sense and antisense primers replacing the codon for Cys with that for Ala (first PCR), as described in the previous papers (14, 15). After the second PCR was performed using universal primers, the amplified fragments (1330 bp) were digested with *Bam*HI and *Pst*II. The digested fragments were ligated into pQE-32 as the wild type. The mutant HdNIR genes were sequenced and expressed in *E. coli* JM109 to produce a recombinant protein.

Physical Measurements. The electronic absorption and CD spectra were measured at 25 °C with a Shimadzu UV-2200 spectrophotometer and a JASCO J-500A spectropolarimeter, respectively. The EPR spectra were recorded with a JEOL JES-FE1X X-band spectrometer at 77 K. The resonance Raman (RR) spectra were obtained with a JASCO NR-1800 at 25 °C. Laser excitation was provided by a 632.8-nm $\text{He}^+ - \text{Ne}^+$ laser (5 mW), and the spectra were obtained from the accumulated data of 32 times scanning. The copper content was determined with a Nippon Jarrel Ash AA-880 Mark-II atomic absorption spectrophotometer. Cyclic voltametric analyses were carried out under Ar atmosphere at 25.0 °C with a Bioanalytical Systems Model CV-50W voltammetric analyzer. The analyzer was equipped with three electrodes, an Ag/AgCl reference electrode, a gold-wire counter electrode, and a bis(4-pyridyl)disulfide-modified gold working electrode.

Kinetic Analysis of Intermolecular Electron-Transfer Reactions from Reduced Cyt c_{550} to Wild-Type and Mutant HdNIRs. Kinetic analyses of wild-type and mutant HdNIRs with Cyt c_{550} were carried out as follows. The reaction

mixture contained reduced Cyt c_{550} in concentrations of 50–200 μM and 2 mM NaNO_2 in a 0.1 M potassium phosphate buffer (pH 5.5). The reaction was initiated by adding an appropriate amount of the recombinant or mutant to the reaction mixture, and a decrease in the 415-nm absorption band was monitored at 25.0 °C. The molar extinction coefficient ($\epsilon_{415\text{nm}} = 135 \text{ mM}^{-1} \text{ cm}^{-1}$) of reduced Cyt c_{550} (8) was used to calculate the kinetic parameters.

RESULTS AND DISCUSSION

Cloning and Sequencing of HdNIR Gene, and Comparison of the Amino Acid Sequence of HdNIR with Those of Cupredoxins and Common NIRs. To obtain amino acid sequence information on HdNIR, the purified enzyme was digested with BrCN and the peptide mixture was separated by reverse-phase HPLC. The amino acid sequences for 6 peptide fragments, which are underlined in Figure 1,² were determined by a protein sequencer. When the specificity and lowering of codon degeneracy of the PCR primers were taken into consideration, two sequences were selected; one is the N-terminal sequence, and the other is the sequence containing conserved copper ligand residues. Thus, two mixed oligonucleotide primers, P1 and P2, were designed and synthesized. A ca. 700-bp fragment that involves a region translatable to four partial amino acid sequences (~P1–P4) could be amplified by PCR using the *H. denitrificans* genomic DNA as a template. Therefore, using the amplified fragment as a specific probe, the HdNIR gene was screened from a partial genomic library of DNA fragments (ca. 6 kbp) obtained by digestion with *Hind*III and then was inserted in pUC19. Finally, one positive clone containing a 5.5-kbp insert was obtained, and the partial nucleotide sequence (3.7 kbp) of the insert was determined in both directions with a DNA sequencer.

The nucleotide sequence located 153 bp downstream of the *Hind*III site is the N-terminal sequence of mature HdNIR, D-A-P-A-M-K-D-K-. Four ATG codons were found in the upstream region of the GAT codon of N-terminal Asp. The potential ribosome-binding sequence (AGGAGGAGA) located 5 bp upstream of the distant codon suggests that the open-reading frame of the HdNIR gene includes 1461 bp encoding 487 amino acid residues. Asp40 is the N terminus of mature HdNIR (calculated $M_r = 48\,167$) and is preceded by the signal peptide of 39 amino acid residues. All of the partial amino acid sequences determined were definitely found in the complete sequence deduced from the nucleotide sequence. No cloned genomic fragment contains the promoter region of HdNIR, but the transcriptional terminator located 25 bp downstream of the termination codon was found.

The open-reading frame of HdNIR is divided into two parts, the N-terminal domain containing a type 1 Cu_N -binding motif (Cys-(X)_a-His-(X)_b-Met) like cupredoxins and C-terminal domain containing a type 1 Cu_C -binding motif having a His ligand (His*) of the type 2 Cu (His*-Cys-(X)_c-His-(X)_d-Met) like common NIRs (Figure 1). We have previously reported that HdNIR is proteolyzed to two protein fragments with subtilisin, the blue Pc-like protein fragment, and the green NIR-like protein fragment (11). That is to say, the protease cleaved between Lys139 and Ser140 residues

² Accession number of the DNA Data Bank of Japan, AB076606 (<http://www.ddbj.nig.ac.jp/>) sequence.

FIGURE 1: Nucleotide and deduced amino acid sequences of *H. denitrificans* nitrite reductase. A possible Shine–Dalgarno (S.D.) sequence is boxed. The transcriptional terminator is shown by arrows. The sequences of peptides obtained by BrCN are underlined. The circled D shows the N-terminal Asp. Putative residues involved in copper coordination are indicated by ● (type 1 Cu_N), ▲ (type 1 Cu_C), and △ (type 2 Cu).

As shown in Figure 2, the N-terminal 92-amino acid sequence (Met40–Leu131) of mature HdNIR is homologous to the amino acid sequences of plastocyanins (30–42% sequence identity); the N-terminal 131-amino acid sequence (Asp1–Leu131) of HdNIR is termed the Pc-like domain of HdNIR. However, the sequence homology of the Pc-like domain to other members of the cupredoxin family is insignificant except for the type 1 Cu-binding motifs; for example, the homology of the Pc-like domain to azurins is about 20%. The type 1 Cu-binding motif containing three ligands in the Pc-like domain, C-S-I-A-G-H-R-Q-A-G-M,

³ The number of Cys, His, and Met residues of the type 1 Cu motif in the previous paper (*II*) should be corrected to 114, 119, and 124, respectively.

HdNIR	38	GRMVIYIGVGGDIDHKIN-P-TLVVHEGETVQVNLVNGEQAQHDVVVDQYAARS---
PC <i>Chlamydomonas</i>	1	DATVKLGADSGALEFVPKTLTIKSGET--VNFVNNAGFPHNIVFDEDAIPSGVN
<i>Chlorella</i>	1	DVTVKLGADSGALVFEPSSVTIKAGET--VTWVNNAGFPHNIVFDEDEVPSTGAN
<i>Enteromorpha</i>	1	AAIVKLGGDDGSLAFVPPNNITVGAGES--IEFINNAGFPHNIVFDEDAVPAGVD
<i>Ulva</i>	1	AQIVKLGGDDGSLAFVPSKISVAAGEA--IEFVNNAGFPHNIVFDEDAVPAGVD
<i>Populus</i>	1	IDVLLGADDGSLAFVPSFESISPGKE--IVFKNNAGFPHNIVFDEDSIPSGVD
HdNIR	89	AI---VNGKNA-SSTFSFVASKVGEFNYYCS*AGHRQAGMEGNIQVL---
PC <i>Chlamydomonas</i>	55	AIS--RDDYLNAPGETYSVKLTAAGEYGYC-EP-HQGAGMVGKIIVQ
<i>Chlorella</i>	55	ALS--HEDYLNAPGESYSKAFDTAGTYGYFC-EP-HQGAGMKGTITVQ
<i>Enteromorpha</i>	55	AIS--AEDYLNASKGQTVVRKLTTPGTGYGYC-DP-HSGAGMKMTITVQ
<i>Ulva</i>	55	AIS--YDDYLNASKGETVVRKLTTPGTGYGYC-EP-HAGAGMKMTITVQ
<i>Populus</i>	54	KISMSEEDLLNAKGETFEVALSNKGEYSFYC-SP-HQGAGMVGVKTVN
CBP	76	---SYFICNFPGHGCSGMKIAVNAL---
Mavicyanin	81	---FYFLCGIPGHGQLGQKVEIKVD---
Rusticyanin	134	---YYYVCQIPGHAATGMFGKIVVK
Auracyanin B	213	---YLYICTFPGHYLAGMKGTLTVP
Azurin	108	---YMFCTFPGH-SALMKGTLTLK
Azurin iso-2	108	---YTYFCSYPGH-FSMRGTLKLEE

Type 1 Cu-binding motif

FIGURE 2: Alignment of the amino acid sequences of the N-terminal 92-amino acid sequence of HdNIR and cupredoxins. The conserved residues of HdNIR and Pc are boxed, and the type 1 Cu ligands are asterisked. Pc: *Chlamydomonas reinhardtii* [SWISS-PROT accession (SP: P25006)], *Chlorella fusca* (SP: P00300), *Enteromorpha prolifera* (SP: P07465), *Ulva pertusa* (SP: P56274), and *Populus nigra* (Popura; SP: P00299). Cupredoxins: cucumber basic protein (CBP; SP: P00303), mavicyanin from zucchini (SP: P80728), azurin from *Pseudomonas aeruginosa* (SP: P00282), azurin iso-2 from *Methylobacterium* sp. J (SP: P12335), and rusticyanin from *Thiobacillus ferrooxidans* (SP: P24930).

seems to lie along a large loop joining the two polypeptide β strands, as observed in cupredoxins (16). In cupredoxins, the copper sites are classified according to the number of residues between the Cys and His ligands and between the His and Met/Gln ligands. The His ligand is solvent-exposed and located in the middle of the large loop distinguished by different lengths and conformations in each cupredoxin (17, 18). In this classification, the type 1 Cu_N site of the Pc-like domain falls into the same category as the Cu sites of CBP (19), auracyanin B (17), rusticyanin (20), stellacyanin (21), and mavicyanin (14); that is, the type 1 Cu-binding motifs of the three cupredoxins show the sequence Cys-(X)₄-His-(X)₄-Met/Gln, although those of plastocyanins exhibit the sequence Cys-(X)₂-His-(X)₄-Met. Moreover, the type 1 Cu sites of the multicopper proteins (laccase, ascorbate oxidase, and ceruloplasmin) also have the sequence Cys-(X)₄-His-(X)₄-Met like the Pc-like domain (22). The amino acid sequence containing the invariant amino acids near the type 1 Cu-binding motifs of 25 plastocyanins is Cys-X-Pro-His-X-Gly-Ala-Gly-Met (16); the two consecutive residues between the ligating His and Met, -Ala-Gly-, are conserved in the Pc-like domain, but a Pro between the Cys and His ligands is not necessarily conserved. With respect to aromatic amino acids around the type 1 Cu, there are Tyr and Phe residues upstream from the Cys ligand. If the position of the Cys is denoted by *n*, both the Pc-like domain and plastocyanins have a Tyr or Phe at positions (*n* - 1) and (*n* - 4).

The C-terminal 284 amino acid sequence (Val164-Gln447) of mature HdNIR is shown in Figure 3 together with the amino acid sequence of the major anaerobically induced outer membrane protein (AniA) containing a type 1 Cu and a type 2 Cu from pathogenic *Neisseria gonorrhoeae* (23), which has no extra type 1 Cu domain at the N terminal. The sequence identity between this Val164-Gln447 domain and five NIRs is as follows: AniA (48%), AcNIR (37%), *Pseudomonas aureofaciens* (PaNIR, 35%), *A. faecalis* (AfNIR,

33%), and AxNIR (32%). It is interesting that the NIR-like domain of HdNIR is very similar to that of AniA. In general, as well as green AcNIR and AfNIR, blue AxNIR and PaNIR show a high level of homology (about 80%), but the blue enzymes show a lower level of homology with the green enzymes (60–70%) (3). The type 1 Cu_C and type 2 Cu motif (His-Cys-(X)₇-His-(X)₄-Met) of the NIR-like domain having the two consecutive His and Cys ligands is also similar to those of AcNIR, AfNIR, AxNIR, and PaNIR, except for the number of amino acid residues between the ligating Cys and His of the type 1 Cu. Although seven amino acid residues between these ligands in AniA are the same as those of the NIR-like domain (Figure 3), AcNIR, AfNIR, AxNIR, and PaNIR have eight residues. The loop of the type 1 Cu motif in the NIR-like domain, together with five NIRs, is longer than those in the Pc-like domain and blue copper proteins (Figure 2). Moreover, the Asp and His residues important for the nitrite reduction activity (6), which are involved in the hydrogen-bond network around the type 2 Cu, are conserved in the amino acid sequence of HdNIR (Asp222 and His365).

Visible Electronic Absorption, EPR, and Raman Spectra of Wild-Type and Mutant HdNIRs. The mutation of HdNIR was performed by PCR mutagenesis. The C114A and C260A mutants were expressed and purified in the same manner as the wild-type enzyme. The ratios of the type 1 Cu to the type 2 Cu in C114A and C260A were estimated to be 1:0.64 and 1:0.68, respectively. The 77-K EPR spectra of these mutants show a set of four hyperfine lines of the type 1 Cu (vide infra), suggesting that the type 1 Cu site with substituted Ala for Cys binds no copper ion.

Like wild-type HdNIR, C260A containing the type 1 Cu_N exhibits a blue color and C114A containing the type 1 Cu_C exhibits a green color. Because wild-type HdNIR has both the type 1 Cu sites, the enzyme possesses a greenish blue color. Figure 4 exhibits the electronic absorption spectra of the two mutants with wild-type HdNIR in a 20 mM

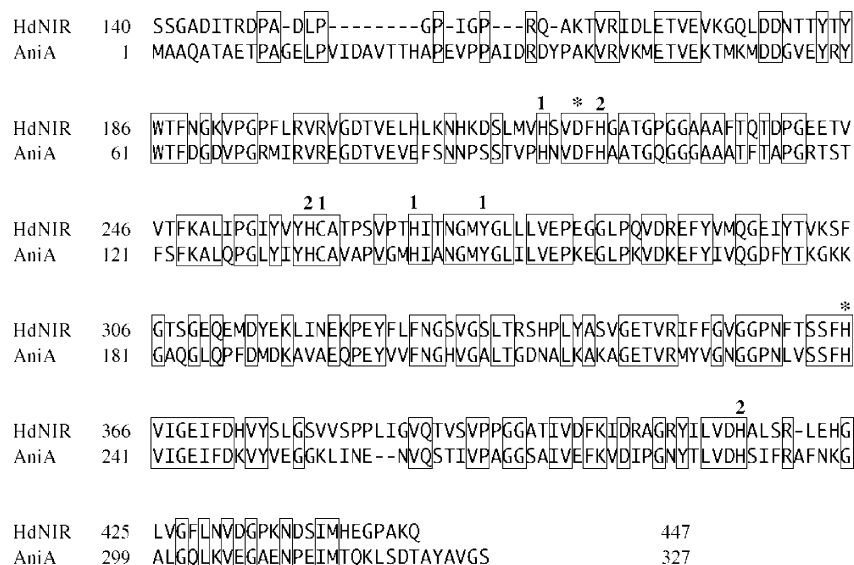


FIGURE 3: Sequence comparison between the NIR-like domain (Ser140–Gln447) of HdNIR and a portion (Met1–Ser327) of *N. gonorrhoeae* NIR (AniA, Gene Bank accession A49208). The numbers 1 and 2 on the sequence indicate the type 1 and type 2 Cu ligands, respectively, and the amino acid residues involved in a hydrogen-bond network around the type 2 Cu are asterisked. Conserved residues are boxed.

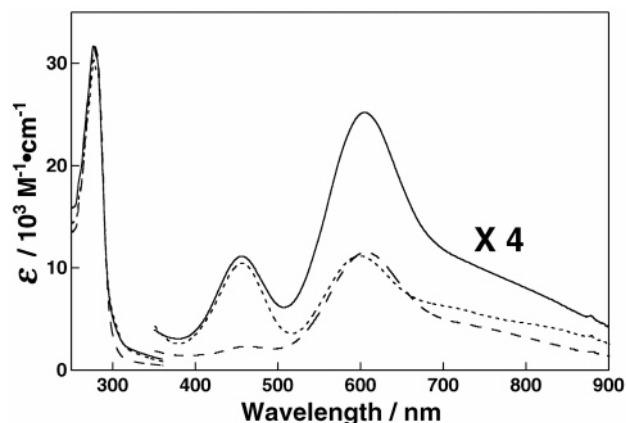


FIGURE 4: UV-visible electronic absorption spectra of wild-type HdNIR (—), C114A (···), and C260A (---) in 20 mM phosphate buffer (pH 7.0).

potassium phosphate buffer (pH 7.0). The absorption peaks [454 ($\epsilon = 2900$) and 605 nm ($\epsilon = 6300 \text{ M}^{-1} \text{ cm}^{-1}$)] of the wild-type enzyme are the same as those of the native enzyme (8). The spectrum of green C114A is clearly distinguishable from that of blue C260A. The sum of the spectra of C114A and C260A is almost equal to the spectrum of HdNIR. The absorption spectrum of C114A showing two peaks at 455 ($\epsilon = 2600$) and 600 nm ($\epsilon = 2800 \text{ M}^{-1} \text{ cm}^{-1}$) and a shoulder near 700 nm in the visible region is analogous to that of the 35-kDa NIR-like protein fragment of HdNIR obtained by a treatment with subtilisin ($\lambda_{\text{max}} = 454$ and 597 nm) (11) and to that of AcNIR ($\lambda_{\text{max}} = 460$, 584, and 690 nm) (13). The spectral pattern of C260A having two peaks at 460 ($\epsilon = 600$) and 605 nm ($\epsilon = 2,900 \text{ M}^{-1} \text{ cm}^{-1}$) resembles those of the 14-kDa Pc-like protein fragment of HdNIR obtained by treating with subtilisin ($\lambda_{\text{max}} = 458$ and 602 nm) (11), AxNIR ($\lambda_{\text{max}} = 470$ and 593 nm) (13), and *Methylomonas* azurin (Az-iso2) ($\lambda_{\text{max}} = 460$ and 616 nm) (24). Moreover, the visible CD spectra of C114A and C260A are also similar to those of the NIR- and Pc-like protein fragments, respectively (11). These electronic absorption and CD spectral data indicate that the type 1 Cu_C site of C114A has a flattened

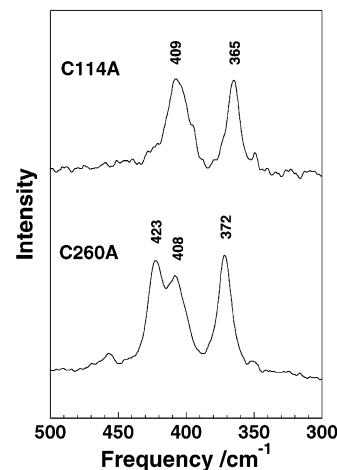


FIGURE 5: RR spectra of C114A and C260A in 0.1 M phosphate buffer (pH 7.0).

tetrahedral geometry like that of AcNIR (25), while the geometry of the type 1 Cu_N of C260A is slightly distorted tetrahedral (or axially elongated bipyramidal) like that of AxNIR (5, 26) [or Az-iso2 (24)].

Excitation of the type 1 Cu proteins within the intense, 600-nm (Cys)S $\rightarrow \text{Cu}^{\text{II}}$ charge-transfer band leads to characteristic RR spectra having several vibrational fundamentals in the region ~ 330 –490 cm^{-1} (27–29). The multiplicity of vibrational modes is believed to originate from kinematic and vibronic coupling of the Cu–S(Cys) stretch with internal ligand deformations of the coplanar (Cys) S_γ –C β –C α –N moiety. Figure 5 compares the typical type 1 Cu resonance Raman spectra of C114A and C260A. Two intense peaks of C114A observed at 409 and 365 cm^{-1} are very similar to those of AcNIR (395 and 361 cm^{-1}) (28), and three intense peaks of C260A at 423, 408, and 372 cm^{-1} resemble those of *A. denitrificans* azurin (429, 411, 398, and 375 cm^{-1}) and *Paracoccus denitrificans* amicyanin (430, 392, and 377 cm^{-1}) (29). In general, the ratio of absorption intensities ($\epsilon_{460\text{nm}}/\epsilon_{600\text{nm}}$) increases with the degree of rhombic distortion (going from trigonal toward tetrahedral geometry) and correlates with an increase in the bond strength of the

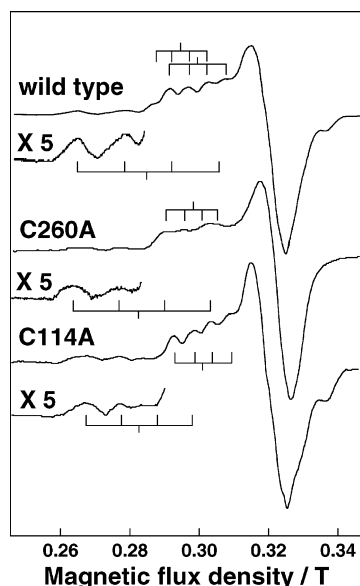


FIGURE 6: X-Band EPR spectra of wild-type HdNIR, C114A, and C260A in 20 mM phosphate buffer (pH 7.0) at 77 K.

axial ligand [Cu–S(Cys) or O(Gln)] in X-ray crystal structures (29–31). Loehr et al. have proposed the correlation of the Cu–S stretching frequency, $\nu_{\text{Cu-S}}$, with the absorbance ratio, $\epsilon_{460\text{nm}}/\epsilon_{600\text{nm}}$, for the type 1 Cu (29). The increased influence of the weak axial ligand upon moving from a trigonal planar (axial EPR) toward a more tetrahedral (rhombic EPR) geometry is associated with a decrease in $\nu_{\text{Cu-S}}$ of the most intense peak from ~ 430 – 405 to ~ 405 – 355 cm^{-1} . The absorbance ratios, $\epsilon_{460\text{nm}}/\epsilon_{600\text{nm}}$, for C260A and C114A, are 0.21 and 0.93, respectively, and the $\nu_{\text{Cu-S}}$ values are 423 and 409 cm^{-1} , respectively. Therefore, the larger absorbance ratio and the smaller $\nu_{\text{Cu-S}}$ of C114A than those of C260A suggest that the type 1 Cu_C moves out of the trigonal ($\text{His})_2(\text{Cys})$ ligand plane and toward the axial ligand compared to the type 1 Cu_N .

In the 77-K EPR spectra of C114A and C260A (Figure 6), the hyperfine structures of the type 1 Cu ions suggest the existence of the only kind of type 1 Cu compared with that of the wild-type HdNIR containing two kinds of the type 1 Cu with the type 2 Cu. The spectrum of C114A consists of a rhombic type 1 Cu_C signal ($g_z = 2.21$ and $A_z = 5.5$ mT) and an axial type 2 Cu signal [$g_{\parallel} = 2.35$ and $A_{\parallel} = 13.5$ mT (8)], resembling that of the NIR-like protein fragment of HdNIR (type 1 Cu, $g_z = 2.21$ and $A_z = 5.0$ mT; type 2 Cu, $g_{\parallel} = 2.31$ and $A_{\parallel} = 14.0$ mT) (11). The EPR spectrum of C260A shows an axial type 1 Cu_N signal ($g_{\parallel} = 2.23$, $A_{\parallel} = 6.0$ mT) with the type 2 Cu signal [$g_{\parallel} = 2.35$, $A_{\parallel} = 13.5$ mT (8)], and the type 1 Cu_N signal is almost the same as that of the Pc-like protein fragment of HdNIR ($g_{\parallel} = 2.23$, $A_{\parallel} = 6.0$ mT) (11). The experimental findings that the type 1 Cu_N and type 1 Cu_C signals display axial and rhombic characters, respectively, are consistent with the results that the geometry of the type 1 Cu_C is more rhombic than that of the type 1 Cu_N according to the RR spectra of C260A and C114A.

Electron-Transfer Reactions of Wild-Type and Mutant HdNIRs from Cyt c_{550} . Our previous study has revealed that a basic electron-transfer heme protein, Cyt c_{550} , is a physiological electron donor for acidic HdNIR (8). The kinetic parameters of wild-type HdNIR and two mutants in the

Table 1: Kinetic Parameters (K_m and k_{cat}) of Wild-Type and Mutant HdNIRs for Cyt c_{550} in the Electron-Transfer Reaction at pH 5.5 and 25.0 °C

enzymes	K_m (μM)	k_{cat} (s^{-1})	k_{cat}/K_m ($\mu\text{M}^{-1} \text{s}^{-1}$)
wild type	31 ± 6	5.8 ± 0.6	0.19
C114A	34 ± 7	5.7 ± 0.8	0.17
C260A	3.0 ± 1.0	$(7.3 \pm 0.1) \times 10^{-3}$	0.0024

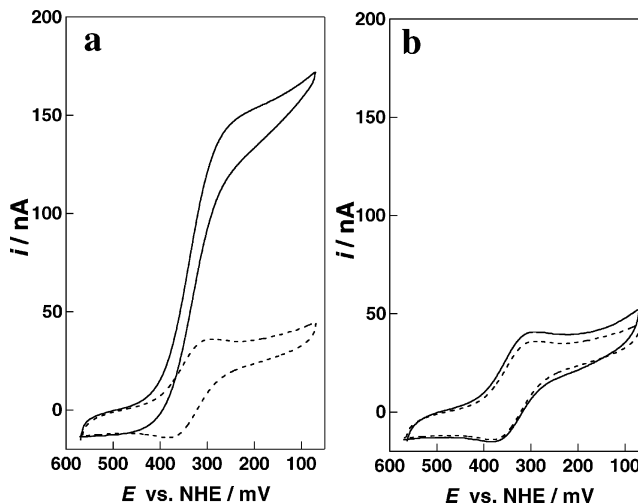


FIGURE 7: Voltammetric behavior of Cyt c_{550} after addition of nitrite (---, a and b) and after addition of nitrite and C114A (—, a) or C260A (—, b) in 0.1 M phosphate buffer (pH 5.5) at 25.0 °C. Cyt c_{550} , 100 μM ; mutant enzymes, 1 μM ; sodium nitrite, 50 μM ; and scan rate, 2 mV/s.

electron-transfer process using Cyt c_{550} are listed in Table 1. The K_m and k_{cat} values of C114A are quite similar to those of wild-type HdNIR, suggesting that the affinity of C114A to Cyt c_{550} is comparable to that of the wild-type enzyme. On the other hand, C260A shows an extremely small k_{cat} and ca. 10% K_m compared to the corresponding values of wild-type HdNIR and C114A. These findings imply that the type 1 Cu_C is essential for the enzyme function and that Cyt c_{550} would interact with the enzyme near the type 1 Cu_C . Consequently, C260A without a type 1 Cu_C shows a very low activity. Because C260A has a stronger affinity for Cyt c_{550} than the wild-type enzyme and C114A, Cyt c_{550} might slowly transfer an electron to the type 2 Cu of C260A.

Electrochemical Studies of Mutant HdNIRs. The cyclic voltammograms of C114A and C260A show well-defined responses with a midpoint potential ($E_{1/2}$) of +321 and +336 mV versus NHE and a peak separation (ΔE) of 79 and 94 mV at pH 7.0, respectively. These cyclic voltammetric responses are due to the type 1 Cu, and the $E_{1/2}$ values are more positively shifted compared to those ($\sim +0.24$ – 0.28 V at pH 7.0) of the type 1 Cu in AxNIR and AcNIR (2, 3). The fact that the $E_{1/2}$ value of the type 1 Cu_C is close to that of the type 1 Cu_N suggests a possibility of the intramolecular electron-transfer reaction between the two type 1 Cu sites. In addition, we have measured the intermolecular electron-transfer reaction from Cyt c_{550} to C114A or C260A in the presence of the nitrite ion in a 0.1 M phosphate buffer (pH 5.5) at 25.0 °C (Figure 7). In this electrochemical reduction of nitrite to NO, the electron-transfer process from a bis(4-pyridyl)disulfide-modified gold working electrode is carried out as follows: electrode \rightarrow Cyt $c_{550} \rightarrow$ type 1 Cu \rightarrow type

2 Cu \rightarrow nitrite. The catalytic current in the presence of C260A was hardly detected, reflecting the slow electron-transfer reaction from Cyt c_{550} to C260A because of the absence of the type 1 Cu_C. On the other hand, the catalytic current was observed when C114A was used instead of C260A. The second-order electron-transfer rate constant for C114A was calculated to be $4.1 \times 10^5 \text{ M}^{-1} \text{ s}^{-1}$. This is similar to those of native HdNIR ($3.7 \times 10^5 \text{ M}^{-1} \text{ s}^{-1}$) (8) and the NIR-like protein fragment ($4.1 \times 10^5 \text{ M}^{-1} \text{ s}^{-1}$) (11) under the same conditions. These rate constants are also similar to those from Cyt c_{551} to AxNIR (10) and from pseudoazurin to AcNIR (9). Thus, the electrochemical behavior of the wild-type and mutant HdNIRs is in accordance with the above results of the electron-transfer reactions of these enzymes.

The direct determination of the midpoint potentials ($E_{1/2}$ versus NHE) at pH 5.5 for Cyt c_{550} and C114A yielded values $E_{1/2}(\text{heme } c) = +366 \text{ mV}$ (9) and $E_{1/2}(\text{T1Cu}) = +321 \text{ mV}$, respectively. Thus, it is expected that no intermolecular electron transfer takes place from Cyt c_{550} to C114A because $E_{1/2}(\text{heme } c)$ is more positive than $E_{1/2}(\text{T1Cu})$. However, the electron transfer actually takes place from Cyt c_{550} to C114A. This could be explained from the catalytic currents shown in Figure 7a, which indicate that the $E_{1/2}$ potentials of Cyt c_{550} and C114A become almost equal because of the conformational changes induced by the interaction between the electron-donor and -acceptor proteins.

CONCLUSIONS

By amino acid sequence analysis, it has been confirmed that HdNIR from a methylotrophic denitrifying bacterium is a new class of NIRs. The 50-kDa HdNIR is composed of two structurally independent domains, a 15-kDa N-terminal domain (Pc-like domain) that has the sequence identity with plastocyanins and a 35-kDa C-terminal domain (NIR-like domain) that has the sequence identity with common NIRs already reported. Each domain possesses a type 1 Cu; the Pc-like domain contains the blue type 1 Cu_N with a $\epsilon_{460\text{nm}}/\epsilon_{600\text{nm}}$ ratio of 0.21 and an axial EPR signal, and the NIR-like domain has the green type 1 Cu_C with a $\epsilon_{460\text{nm}}/\epsilon_{600\text{nm}}$ ratio of 0.93 and a rhombic EPR signal. The geometries of the type 1 Cu_N and Cu_C sites were spectroscopically presumed to be slightly distorted tetrahedral (or axially elongated bipyramidal) and flattened tetrahedral, respectively.

The type 1 Cu_N-depleted mutant (C114A) of HdNIR has almost equal activity in intermolecular electron transfer compared to those of wild-type HdNIR, whereas the type 1 Cu_C-depleted mutant (C260A) shows very low activity. This fact indicates that the type 1 Cu_C site adjacent to the type 2 Cu site is absolutely necessary for the enzyme function of HdNIR. Moreover, the previous paper (11) has reported that the NIR-like protein fragment of HdNIR without the Pc-like domain shows a slightly larger catalytic activity than the wild-type enzyme. It is not clear, at the present stage, what is the role of the Pc-like domain containing the type 1 Cu_N. However, the X-ray crystal analysis and pulse radiolysis of the wild-type and mutant HdNIRs will give an answer to this question, which is in progress.

ACKNOWLEDGMENT

We thank Mr. Mitsuo Ohhama (Osaka University) for RR measurements and Dr. Nobuhumi Nakamura (Tokyo Uni-

versity of Agriculture and Technology) for helpful discussions.

REFERENCES

1. Zumft, W. G. (1997) Cell biology and molecular basis of denitrification, *Microbiol. Mol. Biol. Rev.* 61, 533–616.
2. Suzuki, S., Kataoka, K., and Yamaguchi, K. (2000) Metal coordination and mechanism of multi-copper nitrite reductase, *Acc. Chem. Res.* 33, 728–735.
3. Suzuki, S., Kataoka, K., Yamaguchi, K., Inoue, T., and Kai, Y. (1999) Structure–function relationships of copper-containing nitrite reductases, *Coord. Chem. Rev.* 190–192, 245–265.
4. Adman, E. T., and Murphy, M. E. P. (2001) Copper nitrite reductase, in *Handbook of Metalloproteins* (Messerschmidt, A., Huber, R., Poulos, T., and Wieghardt K., Eds.) Vol. 2, pp 1381–1390, John Wiley and Sons, Chichester, U.K.
5. Inoue, T., Gotowda, M., Deligeer, Kataoka, K., Yamaguchi, K., Suzuki, S., Watanabe, H., Gohow, M., and Kai Y. (1998) Type 1 Cu structure of blue nitrite reductase from *Alcaligenes xylosoxidans* GIFU1051 at 2.05 Å resolution: A comparison between blue and green nitrite reductases, *J. Biochem. (Tokyo)* 124, 876–879.
6. Kataoka, K., Furusawa, H., Takagi, K., Yamaguchi, K., and Suzuki, S. (2000) Functional analysis of conserved aspartate and histidine residues located around the type 2 copper site of copper-containing nitrite reductase, *J. Biochem.* 127, 345–350.
7. Suzuki, S., Kohzuma, T., Shidara, S., Ohki, K., and Aida, T. (1993) Novel spectroscopic aspects of type I copper in *Hyphomicrobium* nitrite reductase, *Inorg. Chim. Acta* 208, 107–109.
8. Deligeer, Fukunaga, R., Kataoka, K., Yamaguchi, K., Kobayashi, K., Tagawa, S., and Suzuki, S. (2002) Spectroscopic and functional characterization of Cu-containing nitrite reductase from *Hyphomicrobium denitrificans* A3151, *J. Inorg. Biochem.* 91, 132–138.
9. Kohzuma, T., Takase, S., Shidara, S., and Suzuki, S. (1993) Electrochemical properties of copper proteins, pseudoazurin, and nitrite reductase from *Achromobacter cycloclastes* IAM 1013, *Chem. Lett.* 1993, 149–152.
10. Deligeer, Kataoka, K., Yamaguchi, K., and Suzuki, S. (2000) Spectroscopic and electrochemical properties of Cytochrome c_{551} from *Alcaligenes xylosoxidans* GIFU 1051, *Bull. Chem. Soc. Jpn.* 73, 1839–1840.
11. Yamaguchi, K., Kobayashi, M., Kataoka, K., and Suzuki, S. (2003) Characterization of two Cu-containing protein fragments obtained by limited proteolysis of *Hyphomicrobium denitrificans* A3151 nitrite reductase, *Biochem. Biophys. Res. Commun.* 300, 36–40.
12. Aida T., and Nomoto, K. (1988) Nitrate removal from a sewage by supplementation of methanol using a submerged soil column, and changes in the population of methanol-utilizing denitrifiers in the column soil, *Jpn. J. Soil Sci. Plant Nutr.* 59, 464–470.
13. Suzuki, S., Deligeer, Yamaguchi, K., Kataoka, K., Kobayashi, K., Tagawa, S., Kohzuma, T., Shidara, S., and Iwasaki, H. (1997) Spectroscopic characterization and intramolecular electron-transfer processes of native and type 2 Cu-depleted nitrite reductases, *J. Biol. Inorg. Chem.* 2, 265–274.
14. Kataoka, K., Nakai, M., Yamaguchi, K., and Suzuki, S. (1998) Gene synthesis, expression, and mutagenesis of zucchini mavi-cyanin: The fourth ligand of blue copper center is Gln, *Biochem. Biophys. Res. Commun.* 250, 409–413.
15. Kataoka, K., Kondo, A., Yamaguchi, K., and Suzuki, S. (2000) Spectroscopic and electrochemical properties of the Met86Gln mutant of *Achromobacter cycloclastes* pseudoazurin, *J. Inorg. Biochem.* 82, 79–84.
16. Sykes, A. G. (1991) Active-site properties of the blue copper proteins in *Advances in Inorganic Chemistry* (Sykes, A. G., Ed.) Vol. 36, pp 377–408, Academic Press, San Diego, CA.
17. Bond, C. S., Blankenship, R. E., Freeman, H. C., Guss, J. M., Maher, M. J., Selvaraj, F. M., Wilce, M. C. J., and Willingham, K. M. (2001) Crystal structure of auracyanin, a “blue” copper protein from the green thermophilic photosynthetic bacterium *Chloroflexus aurantiacus*, *J. Mol. Biol.* 306, 47–67.
18. Donaire, A., Jimenez, B., Fernandez, C. O., Pierattelli, R., Niizeki, T., Moratal, J.-M., Hall, J. F., Kohzuma, T., Hasnain, S. S., and Vila, A. J. (2002) Metal–ligand interplay in blue copper proteins studied by ^1H NMR spectroscopy: Cu(II)-pseudoazurin and Cu(II)-rusticyanin, *J. Am. Chem. Soc.* 124, 13698–13708.

19. Guss, J. M., Merritt, E. A., Phizackerley, R. P., and Freeman, H. C. (1996) The structure of a phytocyanin, the basic blue protein from cucumber, refined at 1.8 Å resolution, *J. Mol. Biol.* 262, 686–705.
20. Walter, R. L., Ealick, S. E., Friedman, A. M., Blake, R. C., II, Proctor, P., and Shoham, M. (1996) Multiple wavelength anomalous diffraction (MAD) crystal structure of rusticyanin: A highly oxidizing cupredoxin with extreme acid stability, *J. Mol. Biol.* 263, 730–751.
21. Nersissian, A. M., Mehrabian, Z. B., Nalbandyan, R. M., Hart, P. J., Fraczkiwicz, G., Czernuszewicz, R. S., Bender, C. J., Peisach, J., Herrmann, R. G., and Valentine, J. S. (1996) Cloning, expression, and spectroscopic characterization of *Cucumis sativus* stellacyanin in its nonglycosylated form, *Protein Sci.* 5, 2184–2192.
22. Messerschmidt, A. (1997) Spatial structures of ascorbate oxidase, laccase, and related proteins: Implications for the catalytic mechanism, in *Multi-copper Oxidases* (Messerschmidt, A., Ed.) pp 23–79, World Scientific Publishing Co. Pte. Ltd, Singapore.
23. Boulanger, M. J., and Murphy, M. E. P. (2002) Crystal structure of the soluble domain of the major anaerobically induced outer membrane protein (AniA) from pathogenic *Neisseria*: A new class of copper-containing nitrite reductases, *J. Mol. Chem.* 315, 1111–1127.
24. Suzuki, S., Nakamura, N., Yamaguchi, K., Kataoka, K., Inoue, T., Nishio, N., Kai, Y., and Tobari, J. (1999) Spectroscopic and electrochemical properties of two azurins (Az-iso1 and Az-iso2) from the obligate methylotroph *Methylomonas* sp. strain J and the structure of novel Az-iso2, *J. Biol. Inorg. Chem.* 4, 749–758.
25. Adman, E. T., Godden, E. J. W., and Turley, S. (1995) The structure of copper-nitrite reductase from *Achromobacter cycloclastes* at five pH values, with NO₂[−] bound and with type II copper depleted, *J. Biol. Chem.* 270, 27458–27474.
26. Dodd, F. E., Hasnain, S. S., Abraham, Z. H. L., Eady, R. R., and Smith, B. E. (1997) Structures of a blue-copper nitrite reductase and its substrate-bound complex, *Acta Crystallogr., Sect. D* 53, 406–418.
27. Han, J., Adman, E. T., Beppu, T., Codd, R., Freeman, H. C., Huq, L., Loehr, T. M., and Sanders-Loehr, J. (1991) Resonance Raman spectra of plastocyanin and pseudoazurin: Evidence for conserved cysteine ligand conformations in cupredoxins (blue copper proteins), *Biochemistry* 30, 10904–10913.
28. Han, J., Loehr, T. M., Lu, Y., Valentine, J. S., Averill, B. A., and Sanders-Loehr, J. (1993) Resonance Raman excitation profiles indicate multiple Cys-Cu charge-transfer transitions in type 1 copper proteins, *J. Am. Chem. Soc.* 115, 4256–4263.
29. Sanders-Loehr, J. (1993) Investigation of type 1 copper site geometry by spectroscopy and molecular design, in *Bioinorganic Chemistry of Copper* (Karlin, K. D., and Tyeklar Z., Eds.) pp 51–63, Chapman and Hall, New York.
30. Andrew, C. R., Yeom, H., Valentine, J. S., Karlsson, B. G., Bonander, N., van Pouderoyen, G., Canters, G. W., Loehr, T. M., and Sanders-Loehr, J. (1994) Raman spectroscopy as an indicator of Cu–S bond length in type 1 and type 2 Copper cysteineate proteins, *J. Am. Chem. Soc.* 116, 11489–11498.
31. Lu, Y., LaCroix, L. B., Lowery, M. D., Solomon, E. I., Bender, C. J., Peisach, J., Roe, J. A., Gralla, E., and Valentine, J. S. (1993) Construction of a blue copper site at the native zinc site of yeast copper–zinc superoxide dismutase, *J. Am. Soc. Chem.* 115, 5907–5918.

BI0492657